The devastating 06.02.2023 Turkey – Syria earthquake of extreme intensity XI: Aposteriori estimates and damage prevention

Anastasia Karakozova[1*], *Sergey* Kuznetsov[1,2], *Vladimir* Mondrus[1], and *Vladimir* Bratov[3]

[1]Moscow State University of Civil Engineering, 26, Yaroslavskoye shosse, Moscow, 129337, Russia
[2]Ishlinsky Institute for Problems in Mechanics, 119526 Moscow, Russia
[3]Edinburgh Napier University, Edinburgh, UK

Abstract. The recent devastating earthquake of M_w7.8 occurred on February 6, 20223 in the Kahramanmaraş region having extreme intensity (XI) on the modified Mercalli scale (MMS) caused the death of more than 52,800 people in Turkey and Syria, as well as severe damages to the infrastructure. The appearance of an unusually strong delta-like S-wave pulse in the seismogram of the main shock and its consequences are analysed, and possible measures to mitigate the possible future high intensity earthquakes are discussed.

1 Introduction

The recent earthquake (06.02.2023) of M_w7.8 and the subsequent strong aftershock M_w7.5, which took place in the Kahramanmaraş region of Turkey and in the nearby regions in Syria, had a relatively shallow hypocentre located within the sedimentary layers of the Earth's crust, about 10,000 meters below the ocean level [1, 2]. The estimated earthquake intensity in the cities Gaziantep and Kilis was XI on the modified Mercalli scale [3, 4]. The aftershocks continue and are likely to continue for about a year after the main shock [3].

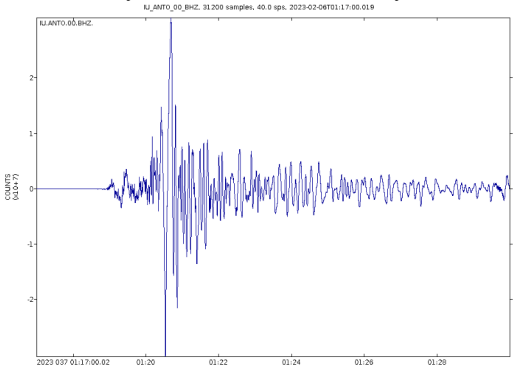

Fig. 1. Seismogram of the main shock at 01:17 GMT, Station IU ANTO, Ankara, Turkey.

* Corresponding author: karioca@mail.ru

The analysis of seismogram detected at different stations reveals the presence of a large delta-like pulse located in Fig. 1 between 01:20 and 01:22. It is apparently associated with the arrival of the horizontally polarized large intensity and short duration S-wave. The authors' estimates indicate the duration of the pulse being ~120 ms. The IU ANTO station is located about 235 km away from the epicentre.

It should also be noted that the situation is much more typical when seismograms recorded at remote stations do not contain large impulses of such a short duration; see a sample of a typical seismogram in Fig. 2.

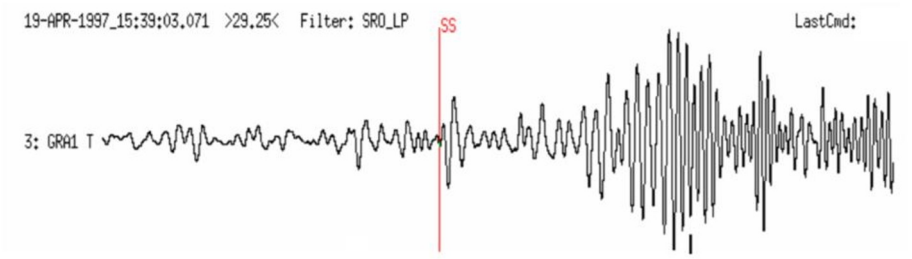

Fig. 2. The typical seismogram; an earthquake near island Severnaya Zemlya, occurred on 19 April 1997 [5]; red line indicates arrival of S-waves.

It should also be noted that the situation is much more typical when seismograms recorded at remote stations do not contain large impulses of such a short duration; see a sample of a typical seismogram in Fig. 2. However, such a short duration and large amplitude pulses were also recorded primarily at the arrival of S-waves accompanying some high intensity earthquakes [6]; see Fig. 3.

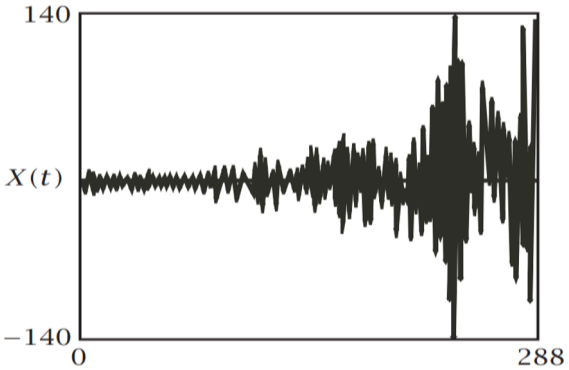

Fig. 3. A seismogram of the Kobe earthquake, occurred on 17 January 1995 [6].

2 What does a delta-like pulse spectrum look like?

Consider integral Fourier transform of a triangle delta-like pulse

$$\tilde{\Delta}(\omega) = \int_{-T}^{T} \Delta(t) \exp\left(-i\omega t\right) dt \qquad (1)$$

where ω is the circular frequency; $\Delta(t)$ is the triangle function having finite support in the time-domain: $\operatorname{supp}\Delta = (-T; T)$

$$\Delta(t) = \frac{p}{T} \times \begin{cases} t+T, & -T < t < 0 \\ T-t, & 0 < t < T \end{cases} \tag{2}$$

In Eq. (1) p is an amplitude multiplier. Applying transformation (1) to function (2), yields

$$\tilde{\Delta}(\omega) = T \cdot \mathrm{sinc}^2\left(\frac{\omega T}{2}\right) \tag{3}$$

where

$$\mathrm{sinc}(t) = \frac{\sin t}{t} \tag{4}$$

In view of (3), the magnitude of $\tilde{\Delta}(\omega)$ becomes; see Fig. 4.

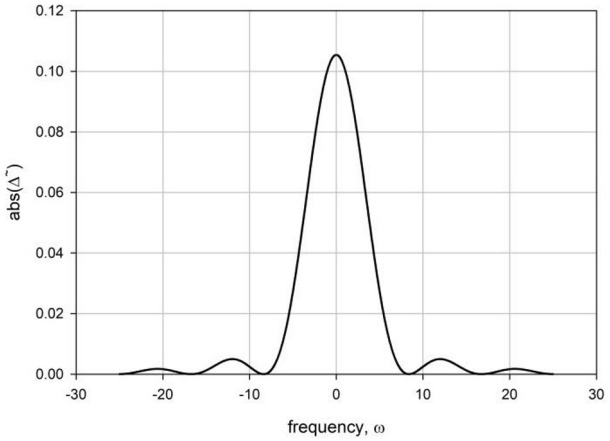

Fig. 4. Fourier spectrum of triangle delta-like pulse.

The plot in Fig. 4 clearly indicates the substantial maximum at zero frequency.

3 AFC of a typical seismic isolating device

Suppose a building is equipped with a typical seismic isolating device, modelled by Kelvin – Voigt model or a more refined Zener model, known also as the standard viscoelastic model [7]. The governing equations for both Kelvin – Voigt and Zener models may be represented in the Cauchy form [8]

$$\frac{d}{dt}\mathbf{Y}(t) = \mathbf{G} \cdot \mathbf{Y}(t) + \mathbf{U}(t) \tag{5}$$

where for Kelvin – Voigt model

$$\mathbf{Y}(t) = \begin{pmatrix} x(t) \\ v(t) \end{pmatrix}; \quad \mathbf{G} = \begin{pmatrix} 0 & 1 \\ -k/m & -\eta/m \end{pmatrix}; \quad \mathbf{U}(t) = \mathbf{U}_0 \exp(i\omega t) \tag{6}$$

Herein, $x(t)$ is the deflection of a mass; $v(t) = \dot{x}(t)$; η is the viscosity of a dashpot; k is the stiffness of a spring; m is the vibration mass; and, $\mathbf{U}_0$ is the amplitude of an external load. Note that $\mathbf{G}$ is a semi-stable matrix [8]. For Zener model with the auxiliary spring, the corresponding parameters become

$$\mathbf{Y}(t) = \begin{pmatrix} x_1(t) \\ x_2(t) \\ v_1(t) \end{pmatrix}; \quad \mathbf{G} = \begin{pmatrix} 0 & 0 & 1 \\ k'/\eta & -k'/\eta & 0 \\ -(k+k')/m & k'/m & 0 \end{pmatrix} \tag{7}$$

where $x_1(t), v_1(t)$ are deflection and speed of the mass; $x_2(t)$ is the deflection of the auxiliary spring; and, k' is the auxiliary spring stiffness.

Solving Eq. (6) at different excitation frequencies yields the amplitude-frequency characteristic (AFC); the typical AFC for Zener model is shown in Fig. 5.

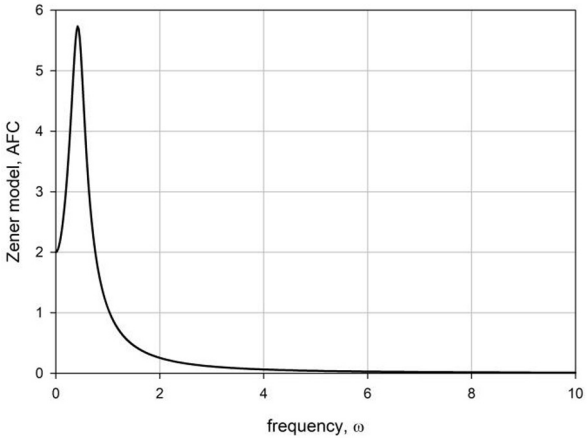

Fig. 5. The typical AFC of a seismic isolating device modelled by a linear Kelvin element

The plot in Fig. 5 clearly demonstrates that the typical seismic isolating device being perfectly suited for damping relatively high frequencies ($\omega > 2$), generates considerable signal amplification in a smaller frequency range ($\omega < 1$), exactly, where the delta-like pulse spectrogram attains its maximum; see Fig. 4. Thus, the considered seismic isolating devices become not only useless at low frequencies, but instead they amplify seismic signals in the low frequency range.

4 Collapse of a frame building without seismic isolation

Consider now the diffraction of the high intensity seismic delta-like S-wave in a frame building without seismic isolation.

The FE analysis of the diffracted large amplitude and short duration S-wave pulse reveals, (i) appearing the high intensity stress fields in both columns and plates; (ii) multiple damage zones mostly appearing at the back-fronts of the diffracted waves; and, (iii) collapse of the frame elements prior to the onset of vibration, when the standing waves are formed; see Fig. 6.

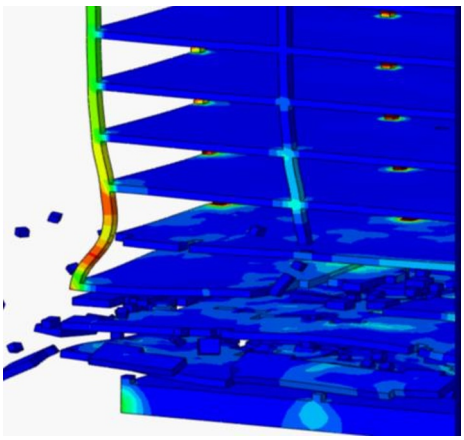

Fig. 6. Collapse of the frame building caused by the arrival of shock waves of high intensity; FE modelling

The slide in Fig. 6 demonstrates collapse of the building frame elements starting from the bottom floors, while the high-intensity wave propagates upward in the building.

5 How to get seismic protection at arrival of high intensity shock waves?

5.1 Seismic pads, an overview

A natural question arises, on how to become seismically protected at the appearance of high intensity and short duration seismic pulses, similar to one appeared in the seismogram of the considered Turkey – Syria earthquake on 06.02.2023; see Fig. 1. That is especially important in view of the principal inability of the seismic isolating devices to damp such short pulses; see Figs. 4 and 5.

Currently, there are several approaches for mitigating the effect the considered shock wave pulses; some of these approaches are already developed, while others are still under development. The already developed solutions include,

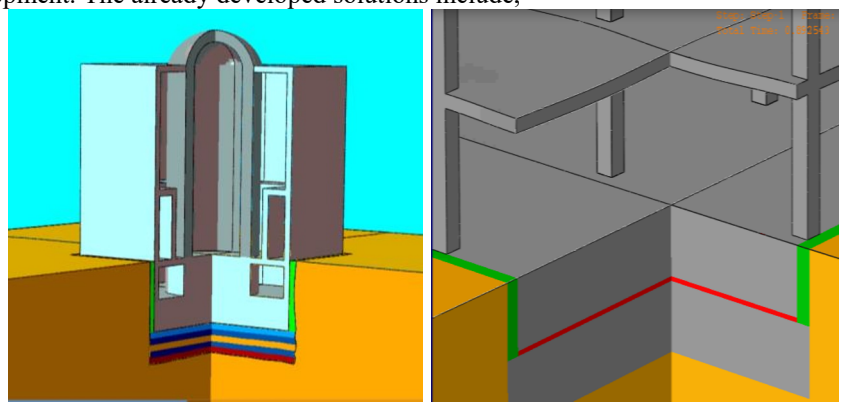

a) b)

Fig. 7. Seismic pads for protecting a) NPP reactor building with a granular seismic pad against both P- and S shock waves below the foundation substructure [9]; b) splitting the grillage with a seismic pad made of granular metamaterial (shown in red) [9].

(I) One of the developed approaches relies on installing a seismic pad beneath the foundation slab (Fig. 7a) or splitting the grillage, in the case of a pile foundation (Fig. 7b); see [9]. These seismic pads are made of granular metamaterials, ensuring (i) reflection of the arriving seismic waves in a broad range of the corresponding spectral frequencies; (ii) absorbing the mechanical energy of seismic waves inside of the granular metamaterial; and (iii) the lifespan of the granular metamaterials comparable or exceeding the lifespan of the protected structure due to the inorganic nature of the granules.

(II) The organic granular materials for applications in the earthquake engineering are also produced [10], however, they generally do not have as long a lifespan, as those made from inorganic materials.

(III) Another solution used at constructing Rion-Antirion bridge and some other long-span bridges [11], consists in a seismic pad made of calibrated natural stones and placed beneath the grillage; the latter is separated from the pile field, ensuring horizontal movement of the grillage and the pylon with respect to the ground.

(IV) Seismic pads especially constructed for seismic isolation of precision equipment, e.g. the use of elastomeric sheets coupled with mechanical sliders [12].

Some other approaches that are currently being under development include,

(V) Seismic pads made of sheets of fluoroplastic, which have a very small friction coefficient and serve for achieving almost friction-free sliding surfaces [13, 14]. This approach can also be referred to the seismic protection by a meta-surface, since it is based on the concept of a sliding surface.

(VI) Seismic pads made of the granular metamaterials and exhibiting properties of the broadband phononic crystals and simulating by the modified Cam-clay model [15]. The main principle of this approach relies on dissipation of mechanical energy inside the pad by using granular materials with low cohesion, which provide the development of plastic deformations at the relative movements of the granules.

5.2 Seismic pads, basic principles

The considered seismic pads are capable for seismic protection from large intensity S-waves in a broad frequency range, moreover, as was previously mentioned, some kinds of pads are capable of protecting from P-waves. At least three basic principles ensuring the efficiency could be stated,

(A) The acoustic impedance difference between ambient soil or concrete and granular metamaterial used for a typical seismic pad (not applicable to seismic pads made of fluoroplastic sheets). This principle ensures reflection of seismic wave energy at the interface between seismic pad and soil or concrete, thus decreasing amount of the wave energy diffracted into building. Note also that the reflection-refraction coefficients do not depend upon wave frequency due to the Knott – Zoeppritz equation.

(B) The appearance of the so called shock wave fronts in the microstructure of the granular material, resulting in the dissipation of the wave energy inside the seismic pad. And, the appeared shock wave fronts are almost insensitive to the diffracted seismic wave frequency.

(C) The ability of relative movement of different granules inside the pad, which ensures attenuation of the seismic wave energy.

6 Concluding remarks

It is noted that the recent devastating earthquake of M_w7.8 occurred on February 6, 20223 in the Kahramanmaraş region and having extreme intensity (XI) on the modified Mercalli scale (MMS) caused the death of more than 52,800 people in Turkey and Syria, as well as severe damages to the infrastructure. Analysis of the seismograms revealed the appearance of an unusually strong delta-like S-wave pulse in the seismogram of the main shock. As was pointed out the observed delta-like pulse corresponds to a large peak located at the zero frequency, making most of the widely used seismic isolating devices almost unusable, or even dangerous, at the appearance of delta-like pulses, since, as was shown, the considered seismic isolators amplify signals in the vicinity of zero frequency.

The analysis of the existing and being under development methods of seismic protection based on different seismic pads containing granular metamaterials, revealed the major benefits of these methods of seismic protection comparing to other types of seismic isolation, especially in regard of the appeared strong delta-like pulses in the earthquake seismograms.

The current research of (A.K., S.K., and V.M.) was supported by the Russian Ministry of Science and Higher Education, grant FSWG-2023-0004.

References

1. USGS, 6 February 2023. "USGS earthquake catalog". Archived from the original on 7 February 2023 (2023).
2. National Earthquake Information Center (6 February 2023). "M 7.8 - 26 km ENE of Nurdağı, Turkey". United States Geological Survey (2023). https://earthquake.usgs.gov/earthquakes/eventpage/us6000jllz/executive
3. Ö. Emre, T.Y. Duman, S. Özalp, et al. Active fault database of Turkey. Bull. Earthquake Eng. **16**, 3229–3275 (2018)
4. V.M. Kawoosa, S. Scarr, Gerry D. (eds.). 10,000 tremors. Reuters. 2 March (2023)
5. P. Bormann, E. Wielandt, Seismic signals and noise. - In: Bormann, P. (Ed.), *New Manual of Seismological Observatory Practice 2 (NMSOP2)*, Potsdam: GFZ, 1-62 (2013)
6. N. Singh, D. Tampubolon, V.S.S. Yadavalli. Time series modelling of the Kobe-Osaka earthquake recordings. Int. J. Math. Math. Sci., **29**(8): 467–479 (2002)
7. R.V. Goldstein et al. Study of forced vibrations of the Kelvin-Voigt model with an asymmetric spring. Mech. Solids, **50**(3): 294–304 (2015)
8. S.V. Kuznetsov. Fundamental and singular solutions of Lamé equations for media with arbitrary elastic anisotropy. Quart. Appl. Math., **63**(3), 455–467 (2005)
9. https://www.marathonalliance.com.au/metamaterials
10. https://www.bridgestone.com/products/diversified
11. O.J. Begambre-Carrillo et al. Passive seismic protection systems with mechanical metamaterials: A current review. Struct. Eng. & Mech., **82**(4): Article 417 (2022)
12. L. Aceto et al. Advances in the optimization design and control of large structures under dynamic loads. In: Eccomas Proceedia COMPDYN, Computational Methods in Structural Dynamics and Earthquake Engineering, M. Papadrakakis, M. Fragiadakis (eds.) 1767-1777 (2021)

13. I. Mirzaev, M. Turdiev. Vibrations of buildings with sliding foundations under real seismic effects, Constr. Unique Build. Struct., 94: Article No 9407 (2021)
14. I. Mirzaev, A. Yuvmitov, M. Turdiev, J. Shomurodov Influence of the vertical earthquake component on the shear vibration of buildings on sliding, E3S Web of Conferences 264, Article No 02022 (2021)
15. R.V. Goldstein et al. The modified Cam-Clay (MCC) model: cyclic kinematic deviatoric loading. Arch. Appl. Mech., **86**(12): 2021–2031 (2016)